REAL TIME DETECTION OF HARMONIC STRUCTURE: A CASE FOR TOPOLOGICAL SIGNAL ANALYSIS

Saba Emrani, Harish Chintakunta and Hamid Krim

Electrical and Computer Engineering Department, North Carolina State University, Raleigh, NC

ABSTRACT

The goal of this study is to find evidence of cyclicity or periodicity in data with low computational complexity and high accuracy. Using delay embeddings, we transform the time-domain signal into a point cloud, whose topology reflects the periodic behavior of the signal. Persistent homology is employed to determine the underlying manifold of the point cloud, and the Euler characteristic provides for a fast computation of topology of the resulting manifold. We apply the introduced approach to breathing sound signals for wheeze detection. Our experiments substantiate the capabilities of the proposed method.

Index Terms— Topological signal analysis, periodicity detection, biomedical signal processing, graph analysis

1. INTRODUCTION

A time series is a collection of data values measured commonly at consecutive uniform intervals of time to reflect particular behavior of a quantity. Detecting periodic patterns in time series can disclose significant information about the behavior and the future trends of the represented entity. The key objective of periodicity detection is finding temporal regularities within the time series to identify whether a complete or almost recurrent structure exists. The problem of discovering potential periods in time series data is an important topic in several audio and image processing applications including speech processing [1], image compression artifacts [2] and patterned texture analysis [3]. Moreover, periodicity detection has been a dynamic area of research in biomedical applications such as DNA and protein sequences and gene regulations [4], [5], [6]. We will demonstrate this application through wheeze detection due to the presence of harmonic content in this type of abnormal breath sounds.

Wheezes are continuous adventitious lung sounds extensively used as an indicator of airway obstruction. The most important characteristic of wheeze signals, which is the key component of this study, is their harmonic behavior. Wheeze detection problem is studied using wavelet and time-frequency techniques in [7], [8] and [9]. We will apply our proposed approach for periodicity detection in wheeze signals for the faster and more accurate performance.

Analysis of data by evaluation of its large scale structure is growing in popularity in the name of topological data analysis [10]. A point cloud includes a large but finite set of points sampled from a primary form. We propose to use time-delay coordinate embedding as a tool to construct a point cloud from a time series. Takens [11] has proved an important theorem which states that almost every time-delay embedding of a time series can recover the underlying dynamics of a system. We can detect the presence of harmonic structures in the data by exploiting topological tools for the analysis of the delay embedding point clouds. Persistent homology is used in [12] to detect topological holes in the delay embedding point cloud occurring on account of the periodic structure of the data. In this paper, we exploit density based subsampling to improve the performance and reduce the number of representative data points. Moreover, Euler characteristics and Delaunay triangulation are utilized to reduce the computational complexity of the algorithm to $O(nlogn)$. Since we describe the global topological structure of the point cloud rather than their local geometric behavior, our approach is robust to missing data points.

The remainder of the paper is organized as follows: the problem modeling and formulation is presented in Section 2. The proposed framework, experimental results and comparison to other methods are included in Section 3. Finally Section 4 concludes the paper.

2. PROBLEM FORMULATION

The proposed signal model is a piecewise sinusoidal function with different periods and phase with a time varying envelope defined as

$$w(t) = \sum_{i=1}^{n} g_i(t), \tag{1}$$

where

$$g_i(t) = \begin{cases} w_i(t) & t_{i-1} \leq t < t_i, \\ 0 & \text{otherwise} \end{cases} \tag{2}$$

and $w_i's, i = 1, 2, ..., n$ are defined as,

$$w_i(t) = A_i \sin\left(\frac{2\pi}{T_i}t + \phi_i\right), A_i \neq 0. \tag{3}$$

Research supported by National Science Foundation EEC-1160483

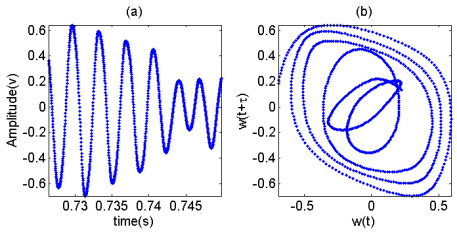

Fig. 1: (a) A short segment of a wheeze signal showing the phase reversal problem (b) its delay embedding

with $\phi_{i+1} = \phi_i + 2\pi t_i \left(\frac{1}{T_i} - \frac{1}{T_{i+1}}\right)$. For each time series $\{w_i\}, i = 1, 2, ..., n$, a two dimensional delay coordinate embedding can be described as the following vector quantity:

$$W(t) = (w(t), w(t+\tau)), \tag{4}$$

where $w(t) \in \mathbb{R}$ and τ is the time delay [11]. It is proved in [12] that the delay-coordinate embedding $W(t)$ is a set of concentric ellipses with angles of rotation $\pm\pi/4$, with varying radii and side lengths of the circumscribed squares around them. It is also shown that $W(t)$ obtained using the appropriate delay always has a topological hole. It also includes a small finite set of points whose coordinates come from different $W_i's$. In fact, these points are created by the transition between neighboring $W_i's$ and are therefore generally close to them. However, since we use a fixed value of delay for different phases, $W(t)$ would include ellipses with both angles of rotations $\pm\pi/4$. Transitioning from one ellipse to another one with different angle of rotation in $W(t)$ happens when a phase reversal takes place in $w(t)$ in time domain. Figure 1(a) illustrates a phase reversal towards the end of a small section of a wheeze signal. The corresponding delay embedding as shown in Figure 1(b), includes two sets of ellipses with angles of rotation $\pm\pi/4$ and the transition points between them. When phase reversal occurs in small amplitudes, the transition points might lie inside the hole, thus "covering" it. The number of these points and their density are very small compared to the total number of points in wheeze signals. This problem is resolved by a subsampling based on the estimated density of the points in section 3.1.

3. PROPOSED FRAMEWORK

3.1. Density Based Point Cloud Subsampling

It is usually the case, as also demonstrated by our experiments, that a very small subset (appropriately sub-sampled) of the data points called landmarks [13] preserves the topology of the data set, thus greatly reducing the computational complexity. The fastest method is random landmark selection that selects the landmarks randomly without replacement. Here, we start with a point cloud X, and choose a smaller set of points $L \subset X$ using this technique. We then apply a density based subsampling to L as described below to eliminate the low density points near the origin caused by phase reversals and improve the performance of the periodicity detection algorithm. A codensity function used in [14] represents the 'nearest neighbor' estimation of the density of the space at each point locally. For each point x in the point cloud X and a fixed positive integer $k > 0$, define $\rho_k(x)$ to be the distance in $\mathbb{R}^2$ from x to its k-th nearest neighbor in X. For each value of k, ρ_k is a metric of the radius of the ball needed to enclose k neighbors. Therefore, $\rho_k(x)$ is inversely proportional to the local density at point x. Different density estimations can be obtained using different values of k. For a fixed k, after sorting the points by their density, we pick a threshold T as the percentage of the points with the highest density ρ_k. The subset of X with the higher T-percent of density can be denoted by $X(k, T)$. If we choose a proper value for k and T, an appropriate representation of the point cloud can be obtained by extracting $X(k, T)$ from X. The analysis of $X(k, T)$ can provide advantageous topological information about the core set around which the data points are accumulated. As discussed in Section 2, in the delay embedding W, there are a fewer number of transition points between ellipses having two different angles of rotation. Once we use random landmark selection on the original point cloud, some of these points appear in the landmarks with a very low probability. Consequently, the topology of the landmarks would be altered by these few number of points. However, the density of these transition points are much lower than the points selected from different $W_i's$. Accordingly, they will not be included in the subsample $W_r(k, T)$ extracted from random landmarks W_r using codensity function.

3.2. Persistent Homology for Parameter Selection

Since our task is to compute the topology of the underlying manifold, our first task is to obtain a triangulation with the vertices in the point cloud whose topology coincides with that of the manifold. This is accomplished by first computing the Delaunay triangulation of the points, and then removing all the "big" edges. Perhaps the most important step of the framework proposed here is in determining this threshold length for the edges in the triangulation. Persistent homology [15], a tool in algebraic topology, is particularly useful in these situations where the "scale" is not known a priori. It may be viewed as a generalization of hierarchical clustering for higher order topological features, which provides a summary, called the barcode, of topology across all scales. Utilizing the barcodes obtained from the sample wheeze and normal breathing signals as our training data, we obtain the appropriate threshold. It also helps in finding appropriate value for (k, T). This process is explained in detail in Seciton 3.4.

3.3. Euler Characteristic for Periodicity Detection

The Euler characteristic $\chi(S)$ for the surface of polyhedra S is given as $V - E + F$ where V, E, and F are the numbers of

vertices, edges and faces in S, respectively. For any topological space, the i-th betti number, $\beta_i, i \geq 0$ intuitively counts the number of i-dimensional holes. For example, β_0 measures the number of connected components, β_1 the number of "holes", etc. The Euler characteristic can also be shown to be equal to $\sum_{i\geq 0}(-1)^i\beta_i(S)$, when the Betti numbers of S are all finite and nonzero only for a finite number of i. Thus,

$$\sum_{i\geq 0}(-1)^i\beta_i(S) = V - E + F \tag{5}$$

In this study the embedding dimension is 2. Therefore, the only Betti numbers that can be nonzero are β_0 and β_1. Moreover, $\beta_0 = 1$ since all the point clouds have only one connected component. Accordingly, equation (5) yields to the following equation for calculating β_1,

$$\beta_1 = 1 - V + E - F \tag{6}$$

Hence, β_1 of the point cloud representing the delay embedding of signals with no cyclicity $n(t)$ and $w(t)$ as defined in (1) are 0 and 1, respectively. We can exploit this fact and equation (6) to detect the periodicity of the time series. In order to find the number of vertices, edges and faces we build a triangle mesh over the vertices of the point cloud. Delaunay triangulation is the natural candidate for this construction. In order to represent the hole inside the point cloud, we then remove the edges longer than a threshold ϵ to be determined using persistent homology. Finally, we can find V, E, F and substitute in equation (6) to find β_1. If $\beta_1 = 1$, the original signal in time domain has almost periodic structure. Otherwise, $\beta_1 = 0$, i.e. there is no cyclicity present in the data.

Using a kd-tree for finding the k-th nearest neighbor, density based subsampling can be performed with $O(mlogm)$ complexity. Since Delaunay triangulation is also an $O(mlogm)$ scheme, the complexity of the whole algorithm would be $O(mlogm)$ where m is the number of landmarks. Accordingly, the proposed algorithm is very fast since the size of the landmark set is extremely smaller than the size of the whole point cloud. Performance and complexity comparison with other methods has been included in the next section to demonstrate the advantages of the proposed technique.

3.4. Experimental Results

The wheeze signal in the time domain resembles that of a sinusoidal wave, justifying their presumed "musicality". Accordingly, we have used the model expressed by Equations (1) to (3) for wheeze signals. We have performed experiments using a large number of recorded breathing sound signals taken from [16], [17] and [18] to support the effectiveness of the proposed approach. The obtained dataset includes 67 signals, 30 normal breathing sounds and 37 wheezes of various types. The sampling rate is 4.41 kHz. For each wheeze signal we choose the interval where wheezes are heard. We then normalize the amplitudes of all the signals between -1 and 1.

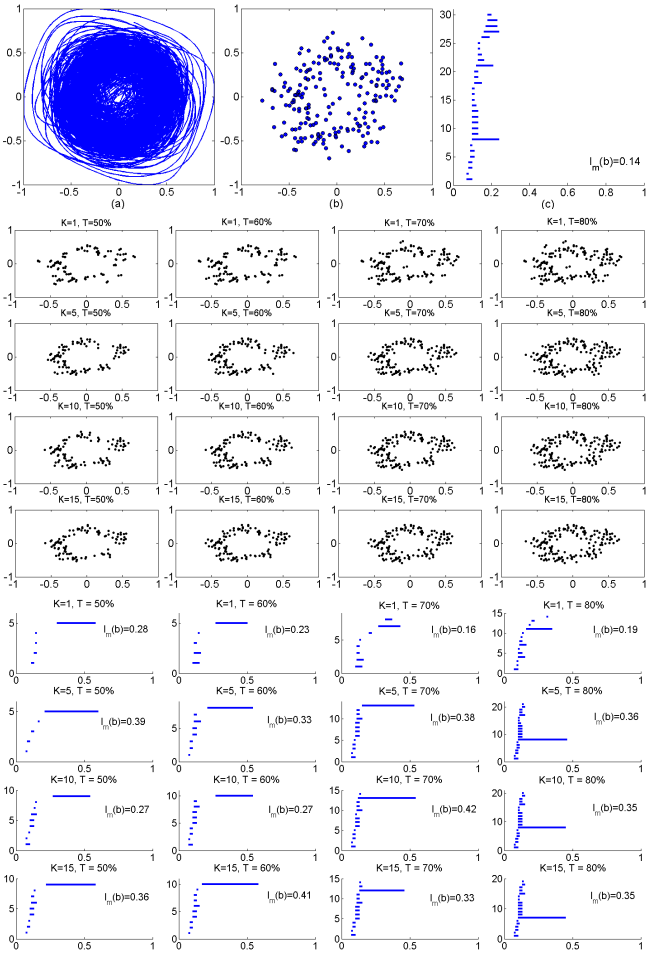

Fig. 2: (top-a) The delay embedding of a wheeze with the phase reversal issue (44,000 points), (b) 200 random landmarks, (c) its barcode, (middle) density based subsamples using different choices of k and T, (bottom) their barcodes with the lengths of the longest bars

Since the size of the dataset is insufficient for straightforward statistical inference, we use a bootstrapping technique to provide more data. For each point cloud, we select 10 different randomly chosen subsets and apply the proposed algorithm to them. Consequently, we validate the performance of the technique using 670 breathing sound data.

Figure 2-(top-a) depicts the delay embedding of 1 second of a wheeze signal including 44000 points. Although the point cloud shows a cyclic behavior due to the periodicity of the signal, the transition points have almost filled the hole inside. Figure 2-(top-b) displays a set of 200 random landmarks selected from (a). Despite the low density of the points near origin in part (a), since the landmarks in (b) are selected randomly there is no hole visible inside them. This is confirmed by the corresponding barcode in Figure 2-(top-c) showing no relatively long persistent interval. However, high

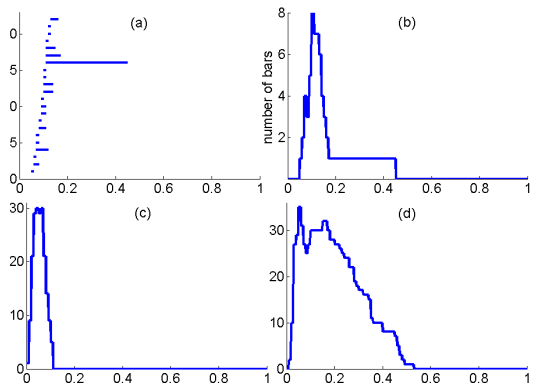

Fig. 3: (a) a barcode selected from Fig. 2, (b) its distribution. (c) the number of point clouds with a hole corresponding to the dataset of non-wheeze signals and (d) wheeze signals

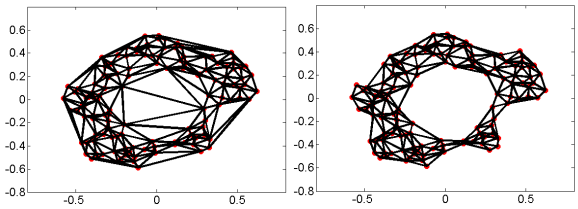

Fig. 4: Delaunay triangulation of a point cloud selected from Fig. 2-(middle) and the corresponding modified triangulation

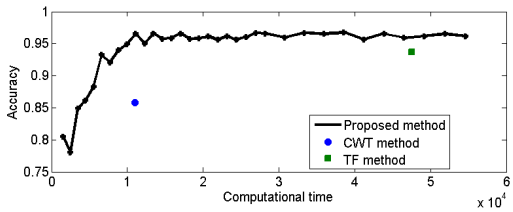

Fig. 5: The performance of the proposed method compared to CWT and TF based techniques

density points are concentrated around a ring with low density points inside and around it. Figure 2-(middle) shows subsamples $W_r(k,T)$ selected out of the random landmarks W_r using the density based method described in section 3.1 using 16 different values for (k,T). For each set of landmarks, the corresponding barcode and the length of the longest persistent interval $l_m(b)$ is computed (Figure 2-(bottom)). This experiment is performed on a small subset of the data and the suitable values of k and T are obtained using averaging such that we get the largest $l_m(b)$ and therefore the biggest hole inside the point cloud. We then exploit the acquired values for the whole data set. To obtain an appropriate value for ϵ, we select two small training sets including signals with and without almost periodic behavior. The barcodes for each data in the selected datasets are calculated as a function of the filtration radius r. For each barcode, we then find the distribution of persistence intervals by calculating the number of bars present at each filtration radius (Figure 3- a,b). Next, for each dataset with cyclicity and without it, we calculate the number of barcodes with nonzero first Betti number as a function of r (Figure 3- c,d). This plot at each filtration radius demonstrates the number of point clouds containing a hole corresponding to the dataset of non-wheeze signals (a) and wheeze signals (b). As it is clear in Figure 3-(bottom), for $\epsilon > 0.11$ there is no barcode with nonzero Betti number in the left plot while there are a high number of them present in the right plot. We chose $\epsilon = 0.16$ to get the maximum difference. The Delaunay triangulation of the obtained subsamples are then constructed and the edges longer than the selected ϵ are eliminated. Figure 4 illustrates this procedure on one of the point clouds shown in Figure 2-(middle) obtained using the selected values of k and T. We then use Euler characteristics as expressed in (6) to calculate β_1.

This algorithm is implemented on all 670 data using different numbers of subsamples for performance evaluation. F measure as the harmonic mean of precision and recall, is used as a measure of accuracy. For each number of the landmarks, the computational complexity and accuracy are calculated and plotted with respect to each other in Figure (5). Previous wheeze detection approaches are mostly based on time frequency(TF) analysis and wavelet transform(WT). The computational complexity of STFT is $O(nlogn)$ while fast CWT can be performed in $O(n)$ time. The TF technique proposed in [19] and WT based method implemented in [19] can also be found in Figure(5). This plot shows how the accuracy and complexity is varying by the size of the subsample while other methods are demonstrated as single points since they use all data samples after subsampling to a fixed frequency. As it is clear in the plot, the computational cost of our technique is much lower than previous methods with a promising performance. Note that the approach proposed in [7] has high computational complexity due to the wavelet bispectrum estimation which is a multidimensional function of two frequencies and is not included in the plot. Additionally, the sensitivity of our method defined as $SE = \frac{TP}{TP+FN}$ using a subsampling factor of 1% is $SE = 98.39\%$ (TP: true posistive, FN: false negative). On the other hand, the sensitivity of the TF techniques proposed in [9], [8] are 95.5% and 86.2%.

4. CONCLUSION

In this study, we proposed a topological method to capture almost harmonic behavior in signals. A promising performance and very low computational complexity is achieved by using density based landmark selection and Euler characteristics. Moreover, since the proposed approach is based on the global topological structure of the point clouds, it is robust to missing data. The experimental result for wheeze detection using a big dataset of lung sounds validate the effectiveness of the introduced algorithm.

5. REFERENCES

[1] O. Deshmukh, C. Y. Espy-Wilson, A. Salomon, and J. Singh, "Use of temporal information: Detection of periodicity, aperiodicity, and pitch in speech," *Speech and Audio Processing, IEEE Transactions on*, vol. 13, no. 5, pp. 776–786, 2005.

[2] Y.-L. Chen and C.-T. Hsu, "Detecting recompression of jpeg images via periodicity analysis of compression artifacts for tampering detection," *Information Forensics and Security, IEEE Transactions on*, vol. 6, no. 2, pp. 396–406, 2011.

[3] H. Ngan and G.-H. Pang, "Regularity analysis for patterned texture inspection," *Automation Science and Engineering, IEEE Transactions on*, vol. 6, no. 1, pp. 131–144, 2009.

[4] J. Tuqan and A. Rushdi, "A dsp approach for finding the codon bias in dna sequences," *Selected Topics in Signal Processing, IEEE Journal of*, vol. 2, no. 3, pp. 343–356, 2008.

[5] N. Song and H. Yan, "Autoregressive and iterative hidden markov models for periodicity detection and solenoid structure recognition in protein sequences," *Biomedical and Health Informatics, IEEE Journal of*, vol. 17, no. 2, pp. 436–441, 2013.

[6] S. Wichert, K. Fokianos, and K. Strimmer, "Identifying periodically expressed transcripts in microarray time series data," *Bioinformatics*, vol. 20, no. 1, pp. 5–20, 2004.

[7] S. Taplidou and L. Hadjileontiadis, "Analysis of wheezes using wavelet higher order spectral features," *Biomedical Engineering, IEEE Transactions on*, vol. 57, no. 7, pp. 1596–1610, 2010.

[8] A. Homs-Corbera, J. Fiz, J. Morera, and R. Jane, "Time-frequency detection and analysis of wheezes during forced exhalation," *Biomedical Engineering, IEEE Transactions on*, vol. 51, no. 1, pp. 182–186, 2004.

[9] S. A. Taplidou and L. J. Hadjileontiadis, "Wheeze detection based on time-frequency analysis of breath sounds," *Computers in Biology and Medicine*, vol. 37, no. 8, pp. 1073 – 1083, 2007.

[10] H. Edelsbrunner and J. Harer, *Computational Topology, An Introduction*. American Mathematical Society, 2010.

[11] F. Takens, "Detecting strange attractors in turbulence," in *Dynamical Systems and Turbulence*, vol. 898 of *Lecture Notes in Mathematics*, pp. 366–381, 1981.

[12] S. Emrani, T. Gentimis, and H. Krim, "Persistent homology of delay embeddings and its application to wheeze detection," *Signal Processing Letters, IEEE*, vol. 21, pp. 459–463, April 2014.

[13] V. De Silva and G. Carlsson, "Topological estimation using witness complexes," in *The First Eurographics conference on Point-Based Graphics*, pp. 157–166, 2004.

[14] G. Carlsson, T. Ishkhanov, V. D. Silva, and A. Zomorodian, "On the local behavior of spaces of natural images," *Internat. J. Comput. Vision*, vol. 76, pp. 1–12, 2008.

[15] H. Edelsbrunner, D. Letscher, and A. Zomorodian, "Topological persistence and simplification," in *Foundations of Computer Science, Proceedings. 41st Annual Symposium on*, pp. 454–463, 2000.

[16] Lippincott Williams and Wilkins, *Auscultation Skills: Breath and Heart Sounds*. Princeton University Press, 2009.

[17] D. Wrigley, *Heart and Lung Sounds Reference Library*. PESI HealthCare, 2011.

[18] R. Wilkins, J. Hodgkin, and B. Lopez, *Fundamentals of Lung and Heart Sounds*. Mosby, 2004.

[19] F. Jin, S. Krishnan, and F. Sattar, "Adventitious sounds identification and extraction using temporal spectral dominance based features," *Biomedical Engineering, IEEE Transactions on*, vol. 58, no. 11, pp. 3078–3087, 2011.